



Refinements to the Q-law for low-thrust orbit transfers

Anastassios E. Petropoulos

Senior Member of the Engineering Staff

Jet Propulsion Laboratory,
California Institute of Technology,
Pasadena, CA 91109-8099, USA.

15th AAS/AIAA Space Flight Mechanics Conference

Copper Mountain, Colorado, January 23–27, 2005
AAS Publications Office, P.O. Box 28130, San Diego, CA 92198

REFINEMENTS TO THE Q-LAW FOR LOW-THRUST ORBIT TRANSFERS

Anastassios E. Petropoulos*

We consider low-thrust orbit transfers around a central body, where specified changes are sought in the orbit elements except true anomaly. The desired changes in the five elements can be arbitrarily large. The Q-law is a Lyapunov feedback control law developed by the author, based on analytic expressions for maximum rates of change of the orbit elements and the desired changes in the elements. Q , the proximity quotient, serves as a candidate Lyapunov function. Three refinements to the Q-law are presented here. First, the concept of relative effectivity, rather than absolute, is introduced for deciding whether to thrust or to coast at any particular point on the transfer. Second, a mechanism is introduced to avoid chatter in the thrust direction when the spacecraft is very near the target orbit and is in an unfavourable location on the osculating orbit. Third, for changing the argument of periapsis, the beneficial effect of out-of-plane thrust, particularly as inclination approaches 0 or 180 degrees, is better utilised. The first two refinements are primarily of use for circle-to-circle transfers, while the latter refinement is of use in orbit transfers involving changes in the argument off periapsis. Two sample orbit transfers demonstrate the utility of the refinements. As before, the Q-law permits a rapid evaluation of the trade-off between propellant mass and flight time, provides reasonable estimates of the flight path and performance of optimal orbit transfers, and also serves as a mechanism for recovering from flight-path disturbances.

INTRODUCTION

The problem of computing many-revolution, low-thrust orbit transfers around a central body is a difficult one; its study began at least as early as the 1950s^{1,2} and continues today. Much of the work has focused on finding propellant-optimal trajectories using either indirect or direct techniques or mixtures of the two, as recently exemplified by Refs. [3–6], [7,8], and [9,10], respectively. Given the dearth of analytic solutions to the optimisation problem, and the difficulty of computing optimal solutions, some attention has also been focused on heuristic control laws. The advantage of the heuristics lies in the speed of computation, which can be orders of magnitude greater than that for optimisation, while the drawback is that the solutions are non-optimal. One category of heuristics^{11–13} involves “blending” the instantaneously optimal thrust directions for changing each of the orbit elements during each of several phases of the orbit transfer. The precise nature of the blending and the delineation of the phases is guided by experience of the mission designer and perhaps by optimisation of the parameters in the control scheme. A second category of heuristics^{13–16} is based on Lyapunov feedback control, where a suitable Lyapunov function must be defined by the mission designer.

In this paper, we refine the Lyapunov feedback control law of Ref. [14] (the Q-law), with the aim of improving approximations to, and good initial guesses for, propellant-optimal, low-thrust orbit transfers which involve specified changes in all orbit elements except true anomaly. In Ref. [13], the candidate Lyapunov function, termed the “proximity quotient,” Q , did not adequately capture the

*Senior Member of the Engineering Staff, Jet Propulsion Laboratory, California Institute of Technology, Pasadena, CA 91109-8099, USA. Member AAS. Member AIAA. Email: Anastassios.Petropoulos@jpl.nasa.gov Copyright © 2005 by Anastassios E. Petropoulos. Published by the American Astronautical Society with permission.

utility of decreasing inclination to decrease the difficulty of making changes in argument of periapsis. The present work presents a method for capturing this utility. The present work also introduces the concept of relative effectivity, rather than absolute, for deciding whether to thrust or to coast at any particular point on the transfer. Also introduced is a mechanism to avoid chatter in the thrust direction when the spacecraft is very near the target orbit and is in an unfavourable location on the osculating orbit. The refined Q-law again has but few input parameters, yet captures the complexity of a wide variety of orbit transfers, including those involving multiple coast arcs.

We present a two orbit transfers computed using the refined Q-law and compare them to results using the previous Q-law.¹⁴ some of these to optimal orbit transfers. A description of the Q-law algorithm is reproduced from Ref. [14], with the above-mentioned refinements introduced at the appropriate points.

Both continuous and intermittent thrusting is permitted for the transfer, but no constraints are placed on when thrusting can occur. When non-zero, the thrust is assumed to be constant, and the specific impulse is similarly constant. The Q-law, as currently formulated, does not attempt to capitalise on the increasing thrust acceleration — the increase will often be of small utility for high specific-impulse missions. The current Q-law logic is oblivious to thruster characteristics and simply provides a thrust direction on the osculating orbit, and an indication of whether to thrust or not. The central body is modelled as a point mass, and the initial and final orbits are assumed closed. No perturbing forces are considered, although the Q-law can be used to rectify changes in the orbit caused by perturbations.

THE Q-LAW ALGORITHM

Definition of the proximity quotient, Q

The proximity quotient, Q , which serves as a candidate Lyapunov function, attempts to judiciously quantify the proximity of the osculating orbit to the target orbit. Q is defined as follows:

$$Q = (1 + W_P P) \sum_{\alpha} W_{\alpha} S_{\alpha} \left[\frac{d(\alpha, \alpha_T)}{\tilde{\alpha}_{xx}} \right]^2, \quad \text{for } \alpha = a, e, i, \omega, \Omega \quad (1)$$

where the five orbital elements (α) are the semimajor axis (a), eccentricity (e), inclination (i), argument of periapsis (ω), and longitude of the ascending node (Ω); W_P and the W_{α} are scalar weights greater than or equal to zero; the subscript T denotes the target orbit element value (without subscript, the osculating value is indicated); $\tilde{\alpha}_{xx}$ nominally (see Eq. 11) denotes the maximum over thrust direction and over true anomaly on the osculating orbit of the rate of change of the orbit element (due to thrust); P is a penalty function; S_{α} is a scaling function; and $d(\alpha, \alpha_T)$ is a distance function. The penalty function is used in the present paper to enforce minimum-periapsis-radius constraints and takes the form

$$P = \exp \left[k \left(1 - \frac{r_p}{r_{p\min}} \right) \right] \quad (2)$$

where k is a scalar, r_p is the osculating periapsis radius, and $r_{p\min}$ is near or equal to the lowest permissible value of r_p . The scaling function is used primarily to prevent non-convergence to the target orbit and takes the form

$$S_{\alpha} = \begin{cases} \left[1 + \left(\frac{a - a_T}{ma_T} \right)^n \right]^{\frac{1}{r}} & \text{for } \alpha = a \\ 1 & \text{for } \alpha = e, i, \omega, \Omega \end{cases} \quad (3)$$

where m, n , and r are scalars with nominal values of 3, 4, and 2, respectively. The distance function is defined as

$$d(\alpha, \alpha_T) = \begin{cases} \alpha - \alpha_T & \text{for } \alpha = a, e, i \\ \cos^{-1} [\cos(\alpha - \alpha_T)] & \text{for } \alpha = \omega, \Omega \end{cases} \quad (4)$$

where the principal value, namely $[0, \pi]$, is used for the arc cosine. The peculiar form of the distance function for ω and Ω is used because it provides an angular measure of the distance between two positions on a circle using the “short way round” the circle, because it is differentiable with respect to α [except when $d(\alpha, \alpha_T) = \pi$], and because the sign of the derivative indicates whether α leads or lags α_T based on the short way round.

Analytic expressions for the $\tilde{\alpha}_{xx}$

Analytic expressions are available¹³ for the maximum rates of change achievable for each of the orbit elements both over the true anomaly on the osculating orbit and over the thrust direction, although for the argument of periapsis analytic expressions are only available if the in-plane and out-of-plane motions are each considered individually. For convenience, a summary of the derivations is presented here. We commence with Gauss’s form of the variational equations for the orbit:¹⁷

$$\frac{d\Omega}{dt} = \frac{r \sin(\theta + \omega)}{h \sin i} f_h \quad (5)$$

$$\frac{di}{dt} = \frac{r \cos(\theta + \omega)}{h} f_h \quad (6)$$

$$\frac{d\omega}{dt} = \frac{1}{eh} [-p \cos \theta f_r + (p + r) \sin \theta f_\theta] - \frac{r \sin(\theta + \omega) \cos i}{h \sin i} f_h \quad (7)$$

$$\frac{da}{dt} = \frac{2a^2}{h} \left(e \sin \theta f_r + \frac{p}{r} f_\theta \right) \quad (8)$$

$$\frac{de}{dt} = \frac{1}{h} \{ p \sin \theta f_r + [(p + r) \cos \theta + re] f_\theta \} \quad (9)$$

$$\frac{d\theta}{dt} = \frac{h}{r^2} + \frac{1}{eh} [p \cos \theta f_r - (p + r) \sin \theta f_\theta] \quad (10)$$

where t is time; θ is true anomaly; p is the semilatus rectum; h is the specific orbital angular momentum; r is the radius from the central body, related to the osculating elements through the conic equation $r = p/(1 + e \cos \theta)$; and f_r , f_θ , and f_h are the components of the thrust acceleration in the radial, circumferential and angular momentum directions, respectively. Using the thrust angles α (measured in the orbit plane off of the circumferential direction, positive away from the gravitational centre) and β (measured off of the orbit plane and perpendicular to it, positive in the direction of the angular momentum), the thrust acceleration components are given as:

$$\begin{aligned} f_r &= f \cos \beta \sin \alpha \\ f_\theta &= f \cos \beta \cos \alpha \\ f_h &= f \sin \beta \end{aligned}$$

The following definition is used for $\tilde{\alpha}_{xx}$,

$$\tilde{\alpha}_{xx} = \begin{cases} \dot{\alpha}_{xx} = \max_{\alpha, \beta, \theta} (\dot{\alpha}) & \text{for } \alpha = a, e, i, \Omega \\ (\dot{\omega}_{xxi} + b\dot{\omega}_{xxo})/(1 + b) & \text{for } \alpha = \omega \end{cases} \quad (11)$$

where b is a non-negative constant, nominally taken as 0.01, and

$$\dot{\omega}_{xxi} = \max_{\alpha, \theta} \left(\dot{\alpha} \Big|_{\beta=0} \right) \quad (12)$$

$$\dot{\omega}_{xxo} = \max_{\theta} \left(\dot{\alpha} \Big|_{\beta=\pi/2} \right) \quad (13)$$

are the maximum rates of change for ω when purely in-plane thrust is applied, or when purely out-of-plane thrust is applied, respectively. The previous definition of the Q-law¹⁴ did not contain the second term in the sum shown in Eq. 11, *i.e.*, the previous definition is recovered if b is here set to zero. Now, using f for the thrust-acceleration magnitude and μ for the gravitational parameter of the central body, there arises for the semimajor axis:

$$\dot{a}_{\text{xx}} = 2f \sqrt{\frac{a^3(1+e)}{\mu(1-e)}} \quad (14)$$

and for the eccentricity:

$$\dot{e}_{\text{xx}} = \frac{2pf}{h} \quad (15)$$

and for the inclination:

$$\dot{i}_{\text{xx}} = \frac{pf}{h \left(\sqrt{1 - e^2 \sin^2 \omega} - e |\cos \omega| \right)} \quad (16)$$

and for the longitude of the ascending node:

$$\dot{\Omega}_{\text{xx}} = \frac{pf}{h \sin i \left(\sqrt{1 - e^2 \cos^2 \omega} - e |\sin \omega| \right)} \quad (17)$$

and for the argument of periapsis with purely in-plane thrust:

$$\dot{\omega}_{\text{xxi}} = \frac{f}{eh} \sqrt{p^2 \cos^2 \theta_{\text{xx}} + (p + r_{\text{xx}})^2 \sin^2 \theta_{\text{xx}}} \quad (18)$$

where

$$\cos \theta_{\text{xx}} = \left[\frac{1 - e^2}{2e^3} + \sqrt{\frac{1}{4} \left(\frac{1 - e^2}{e^3} \right)^2 + \frac{1}{27}} \right]^{\frac{1}{3}} - \left[-\frac{1 - e^2}{2e^3} + \sqrt{\frac{1}{4} \left(\frac{1 - e^2}{e^3} \right)^2 + \frac{1}{27}} \right]^{\frac{1}{3}} - \frac{1}{e} \quad (19)$$

$$r_{\text{xx}} = \frac{p}{1 + e \cos \theta_{\text{xx}}} \quad (20)$$

and for the argument of periapsis with purely out-of-plane thrust:

$$\dot{\omega}_{\text{xxo}} = \dot{\Omega}_{\text{xx}} |\cos i| \quad (21)$$

Discussion of the Q-law and effectivity

It is clear from the definition of the proximity quotient in Eq. 1 that Q is zero at the target orbit and positive elsewhere. Thus, our goal in the orbit transfer is to drive Q to zero. Q may be thought of as a “best-case quadratic time-to-go,” in that it captures the best possible rate of change for each of the orbit elements over the osculating orbit — the ratio $|d(\alpha, \alpha_T)/\dot{\alpha}_{\text{xx}}|$ is the time it would take to reach the target value for that α if this best possible rate of change could be sustained throughout the transfer. We note that Q is a function only of the five orbit elements, and not of true anomaly or the thrust angles. The summation in Eq. (1) is available analytically since analytic expressions have been derived for each of the $\dot{\alpha}_{\text{xx}}$. Now, the time rate of change of Q is simply

$$\frac{dQ}{dt} = \sum_{\alpha} \frac{\partial Q}{\partial \alpha} \dot{\alpha} \quad (22)$$

where each of the \dot{a} are available explicitly from the variational equations (5)–(9). Thus, unlike Q , \dot{Q} depends on the thrust angles. At any point on the transfer, we choose the thrust angles, α_n and β_n , which make \dot{Q} most negative:

$$\dot{Q}_n = \min_{\alpha, \beta} \dot{Q} \quad (23)$$

\dot{Q}_n is always less zero. The angles α_n and β_n that minimise \dot{Q} are available analytically. The Q-law uses these thrust angles, thereby ensuring that Q is being sent towards zero as quickly as possible at each instant. From the functional form of Q , we see that reducing Q might involve not only reducing $d(\varpi, \varpi_T)$, but also increasing \dot{a}_{xx} . Sacrificial changes in one orbit element can thus be made [increasing $d(\varpi_1, \varpi_{1T})$], if other elements can then be changed more easily (increasing \dot{a}_{2xx}). This sort of balancing between orbit elements is akin to the classic example of a large plane change for a circular orbit: The propellant-optimal way to accomplish this is to enlarge the orbit, making the plane change easier, and then to shrink the orbit back to its original size.

One complication that is difficult to address analytically is that of convergence. Although we can always apply thrust so as to reduce Q , since $\dot{Q}_n < 0$, we have not proved that doing so will always drive the orbit elements to their target values. For example, if we replace the scaling coefficient of Eq. 3 with $S_a = 1$, we see that Q becomes zero not only at the target orbit, but also at $a = \infty$, which would prevent some initial orbits from converging to the target orbit (converging instead to $a = \infty$). However, for the nominal Q of Eq. 1, convergence has been seen over all of the wide range of orbit transfers studied numerically so far.

While the thrust angles α_n and β_n ensure the optimal rate of reduction of Q at the current true anomaly, they do not provide any information about how effective the thrust is, as compared with other locations on the osculating orbit. Thus, it is natural to define the absolute effectivity of the thrust at the current true anomaly as

$$\eta_a = \frac{\dot{Q}_n}{\dot{Q}_{nn}} \quad (24)$$

and the relative effectivity as

$$\eta_r = \frac{\dot{Q}_n - \dot{Q}_{nx}}{\dot{Q}_{nn} - \dot{Q}_{nx}} \quad (25)$$

where

$$\dot{Q}_{nn} = \min_{\theta} \dot{Q}_n \quad (26)$$

$$\dot{Q}_{nx} = \max_{\theta} \dot{Q}_n \quad (27)$$

$$(28)$$

In the previous Q-law,¹⁴ only the absolute effectivity was used. A mission designer may then chose to prevent the spacecraft from thrusting if the absolute effectivity is below some cut-off value, $\eta_{a \text{ cut}}$ and/or if the relative effectivity is below some cut-off value, $\eta_{r \text{ cut}}$. Broadly speaking, the greater the cut-off, the greater the expected propellant savings and the longer the expected flight time. An analytic expression is not available for \dot{Q}_{nn} , and so this value must be computed numerically — an approximate value is normally sufficient, and so the computational burden is very slight. The relative effectivity is suited to planar transfers involving circular orbits, since the absolute effectivity will be close to unity around the whole orbit.

Also introduced in this paper is the idea of switching to a higher absolute effectivity cut-off when the osculating orbit comes very near the target orbit and the absolute effectivity is low. For planar, circle-to-circle transfers, this is useful because the spacecraft often arrives near the target orbit at an unfavourable location on the osculating orbit. For example, the spacecraft may be at apoapsis, with acquisition of the target orbit requiring a miniscule increase in semimajor axis, but also a miniscule decrease in eccentricity. The thrust directions to accomplish these changes whilst

at apoapsis are diametrically opposed, and so the absolute effectivity is very low. Chatter in the thrust direction will often arise in this situation. A simple method of reaching the target orbit is to turn off the thrust until the vicinity of periapsis is reached. The switch to a higher effectivity accomplishes just that. Using a switch to a higher effectivity is a technique which easily fits directly into the framework of the Q-law and applies to all orbit transfers which might suffer from similar problems, and so has the advantage of not having to develop special criteria for individual cases. Q itself serves as a natural quantity for determining when the osculating orbit is close enough to the target orbit to switch effectivities. For example, when \sqrt{Q} is close to the orbit of the target period, only one or a small number of revolutions are needed to reach the orbit (since, as mentioned earlier, Q is essentially the best-case quadratic time-to-go).

Using the Q-law as a feedback algorithm

In this paper, the orbit transfers are computed by numerically integrating the variational equations 5–9 and the mass-flow-rate equation, where Eq. 8 is replaced by the variational equation for \dot{p} , where the thrust angles are determined by the Q-law, and where the decision of whether to apply thrust or not is based on the Q-law effectivity cut-off. A mission designer specifies the thrust, the specific impulse, initial values for spacecraft mass and $(a, e, i, \omega, \Omega, \theta)$, and final values for the orbit elements of interest (except θ , of course). For any element, ϱ , whose final value is free, the corresponding weight, W_{ϱ} in Eq. 1, is set to zero. The remaining W_{ϱ} are set to non-zero values, nominally unity. A minimum-periapsis-radius constraint is imposed by setting the penalty-function weight, W_P , to be non-zero, nominally unity. The associated parameters k and $r_{p\min}$ in Eq. 2 are normally set in concert with each other — the size of k determines how steeply the exponential barrier rises at $r_p = r_{p\min}$. The numerical integration is performed using a 5th-6th-order Runge-Kutta algorithm, with fixed step size in true longitude.

Due to the use of the classical orbit elements, the Q-law and the variational equations have singularities at zero-inclination and at zero-eccentricity. Thus, initial and target orbits are always specified to be outside of a small region surrounding the singularities. As a rather coarse approximation, in the unlikely event that during the numerical integration the inclination (in radians) or eccentricity try to drop below 10^{-4} , their values are artificially frozen at this value until their rates of change become positive.

RESULTS

Transfers between two pairs of initial and final orbits are studied using the refined Q-law, and compared to results presented in Ref. [14] (i.e. where the previous version of the Q-law was used). (The term orbit transfer is here sometimes used to refer to a particular trajectory joining an initial and final orbit, and sometimes to refer simply to the pair of orbits to be joined by some as-yet undetermined trajectory.) Table 1 lists the orbit transfers and their associated thrust characteristics and central body. In each case, the trade-off between propellant mass and flight time is investigated by varying the effectivity cut-offs. The effectivity cut-offs are considered individually; that is, when using absolute effectivity to determine whether to thrust or coast, the value of the relative effectivity is ignored, and *vice versa*. Trajectory plots and associated data are also presented. For Earth $\mu = 398600.49\text{km}^3/\text{s}^2$. The standard acceleration due to gravity is taken as $9.80665\text{m}/\text{s}^2$.

Unless otherwise noted, nominal values are used for the Q-law parameters: Zero and unity are used for the W_{ϱ} (depending on whether the target value of an element is free or fixed); m, n, r are taken as 3,4,2, respectively; b is taken as 0.01; and W_P is unity when a periapsis constraint is imposed, zero otherwise. The minimum permitted length of a thrust arc is 10° in true longitude (over-riding η_{cut} , if need be), to prevent thrust-on-off chatter around $\eta = \eta_{\text{cut}}$. The initial true anomaly is taken as zero.

Table 1

Orbit Transfers

| Case ^a | Orbit | a (km) | e | i (deg.) | ω (deg.) | Ω (deg.) | Thrust (N) | Initial Mass (kg) | Specific Impulse (s) | Central Body |
|-------------------|-------|-------------|-------|---------------|--------------------|--------------------|---------------|-------------------------|----------------------------|-----------------|
| A | Init. | 7000 | 0.01 | 0.05 | 0 | 0 | 1 | 300 | 3100 | Earth |
| | Targ. | 42000 | 0.01 | free | free | free | | | | |
| E | Init. | 24505.9 | 0.725 | 0.06 | 0 | 0 | 2 | 2000 | 2000 | Earth |
| | Targ. | 26500 | 0.7 | 116 | 270 | 180 | | | | |

^aNon-sequential case designations are used to maintain correspondence with designations in Ref. [14], where five cases were considered.

Case A

Case A is essentially a simple coplanar, circle-to-circle orbit transfer from low Earth orbit to geostationary orbit. No periapsis constraint is imposed during the transfer, as the natural dynamics do not decrease the periapsis altitude. A somewhat-high thrust-to-mass ratio is used so that some detail can still be discerned when the trajectories are plotted. When relative effectivity is used as the cut-off criterion, thrust-direction chatter is avoided near the target orbit by switching to absolute effectivity as a cut-off criterion, with a cut-off value of $\eta_{a\text{ cut}} = 0.8$ when \sqrt{Q} is less than half the period of the target orbit and when $\eta_a \leq 0.7$.

The trade-off between propellant mass and flight time is shown in Fig. 1. The set of points arising from the use of the absolute effectivity cut-off shows a large gap in stepping $\eta_{a\text{ cut}}$ from 0.967 to 0.968. The gap arises because on the very first revolution, the minimum absolute effectivity is between 0.967 and 0.968, and the minimum over each of many subsequent revolutions increases. Thus, only at $\eta_{a\text{ cut}} \geq 0.968$ is a coast arc introduced on the first revolution. Because a small coast arc is introduced near apoapsis on the first revolution, the minimum absolute effectivity over the second revolution now drops below 0.968, which means that another coast arc is introduced, and so on, with the subsequent revolutions. Thus, when the threshold $\eta_{a\text{ cut}} = 0.968$ is passed, many coast arcs are introduced, resulting in a jump in flight time and a reduction in propellant mass. When relative effectivity is used, no large gaps arise in the set of points corresponding to different cut-off values, since with a non-zero cut-off, coast arcs generally introduced on every revolution (around the location where it is least effective to reduce Q). For the relative effectivity case, the unexpected slight increase in propellant mass occurs because of a slight overshoot in semimajor axis. Such overshoots, can be mitigated by adjusting the weights in the Q function.¹⁸ Some characteristics of the Q-law transfers for the various effectivity cut-offs annotated in Fig. 1 are tabulated in Table 2.

As expected, the $\eta_{r\text{ cut}} = 0$ case (which is equivalent to the $\eta_{a\text{ cut}} = 0$) yields the shortest flight time for the Q-law, as thrust is applied continuously. The trajectory, shown in Fig. 2, is roughly a circular spiral. According to Edelbaum’s averaging analysis,² the optimal ΔV for the minimum-time transfer between two coplanar circular orbits is the difference in circular orbit speeds (from which the minimum time can be computed). The Q-law with $\eta_{r\text{ cut}} = 0$ approaches the Edelbaum performance very closely (see Table 2).

At large $\eta_{r\text{ cut}}$ values, the transfer trajectory takes a rather different form, opting to roughly emulate a Hohmann transfer by performing multiple short burns around periapsis or around apoapsis. Of course, the number of revolutions and the flight time are greater than for the minimum time case of $\eta_{r\text{ cut}} = 0$. For intermediate values of $\eta_{r\text{ cut}}$ (and, correspondingly, of flight time and propellant mass), the trajectory geometries look like a blending of the geometries of the extreme

cases of small and large $\eta_{r \text{ cut}}$ values. Figs. 3, 4 and 5 show the trajectories for $\eta_{r \text{ cut}}$ values of 0.167, 0.435 and 0.861, respectively. Table 2 shows that the ΔV requirement for the Q-law transfers closely approaches that of the Hohmann transfer as longer and longer flight times are used.

An instructive way of comparing the transfers corresponding to different $\eta_{r \text{ cut}}$ values is to plot their osculating apoapsis radius, r_a , versus their osculating periapsis radius, r_p , as shown in Fig. 6. The continuous-thrust case of $\eta_{r \text{ cut}} = 0$ is immediately seen to remain close to circular throughout the transfer. In contrast, the long flight-time, propellant-saving cases of $\eta_{r \text{ cut}} = 0.861$ and $\eta_{r \text{ cut}} = 0.933$ maintain a low r_p , making it very effective to add energy (by thrusting near periapsis), until r_a becomes supersynchronous, whereupon the orbit is circularised. As $\eta_{r \text{ cut}}$ is reduced, shortening the flight times, r_p rises more and more quickly in the energy-boosting phase of the transfer, as shown for the $\eta_{r \text{ cut}}$ values of 0.435 and 0.167. Amongst the very high $\eta_{r \text{ cut}}$ values, little difference exists between the paths taken on the r_a - r_p plot (as exemplified by the curves for $\eta_{r \text{ cut}}$ values of 0.861 and 0.933).

The overshoot in apoapsis radius seen in Fig. 6 is due to the fact that eccentricity is most effectively changed at apoapsis, especially the larger the apoapsis radius. The precise size of the overshoot will depend on the particular values chosen for the weights and other constants appearing in the expression for the proximity quotient, Q .¹⁸ Thus, the amount of overshoot, as well as the exact flight-time and propellant performance, can be tweaked by adjusting the values of the weights and constants in Q .

Table 2

Selected orbit transfer solutions for Case A

| Solved by | Flight time (days) | ΔV (km/s) | Propellant Mass (kg) | Revs ^a |
|---------------------------------------|--------------------|-------------------|----------------------|-------------------|
| Q-law, $\eta_{r \text{ cut}} = 0$ | 14.600 | 4.5257 | 41.4953 | 90.38 |
| Q-law, $\eta_{r \text{ cut}} = 0.167$ | 25.687 | 4.6522 | 42.5692 | 131.85 |
| Q-law, $\eta_{r \text{ cut}} = 0.435$ | 37.514 | 4.4651 | 40.9793 | 191.39 |
| Q-law, $\eta_{r \text{ cut}} = 0.861$ | 100.573 | 3.9826 | 36.8354 | 501.87 |
| Q-law, $\eta_{r \text{ cut}} = 0.933$ | 150.701 | 3.9113 | 36.2178 | 747.41 |
| Q-law, $\eta_a \text{ cut} = 0.968$ | 152.389 | 3.9524 | 36.5739 | 666.02 |
| Edelbaum | 14.4199 | 4.4654 | 40.9820 | – |
| Hohmann | 0.22086 | 3.7680 | 34.9717 | 0.5 |

^aRevolutions in true anomaly.

Case E

Case E is a transfer from a geostationary transfer orbit to a retrograde, Molniya-type orbit. The required plane change is about 116°. Target values are set for all five orbit elements. The periapsis-radius penalty function is used with $W_P = 1$, $k = 100$, and $r_{p \text{ min}} = 6578 \text{ km}$. A study of the trade-off between propellant mass and flight time is conducted by varying $\eta_a \text{ cut}$.

When the old definition of Q is used (Ref. [14]), two families of solutions arise. In Fig. 7, which shows the trade-off between propellant mass and flight time, these families are labelled L and M. Family L is much poorer in performance than family M, since it not only consumes more propellant, but also does not include the minimum flight time case. The appearance of the two families is caused by the singularity in the $\dot{\omega}$ variational equation at zero inclination, and by the inability of the old Q-law to take advantage of it explicitly. The old Q-law simply stumbles onto the better-performing solutions due to fortuitous values of $\eta_a \text{ cut}$ which happen to cause thrust to

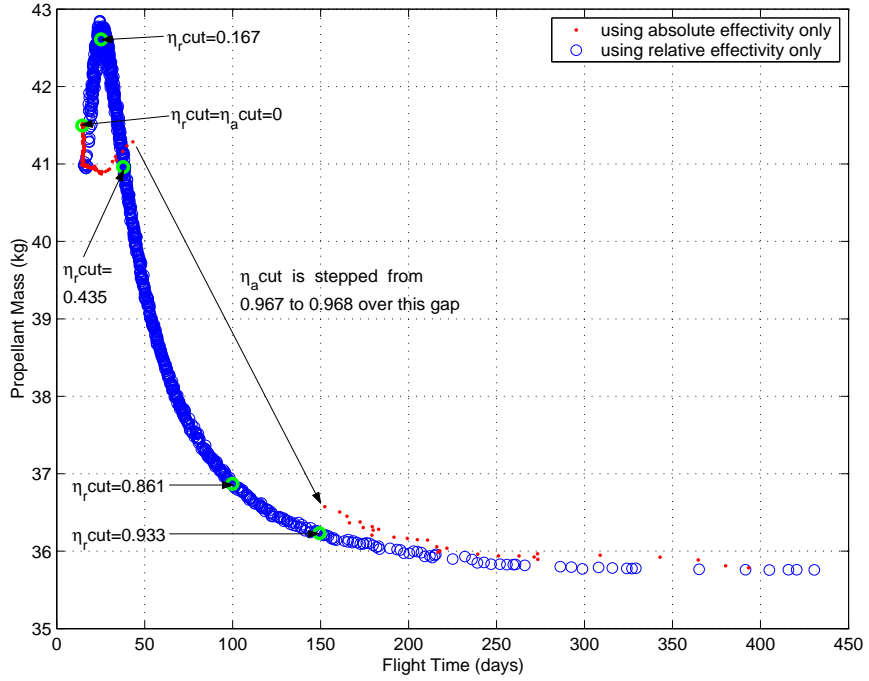


Figure 1 Case A Q-law transfer: Trade-off between propellant mass and flight time, assessed by varying and considering in one instance only the absolute effectivity cut-off ($\eta_{a\text{ cut}}$) and in the other instance only the relative effectivity cut-off ($\eta_{r\text{ cut}}$). The cut-offs are stepped up from zero in increments of 0.001. The largest cut-off values that give flight times short enough to appear on the plot are $\eta_{a\text{ cut}} = 0.996$ and $\eta_{r\text{ cut}} = 0.994$.

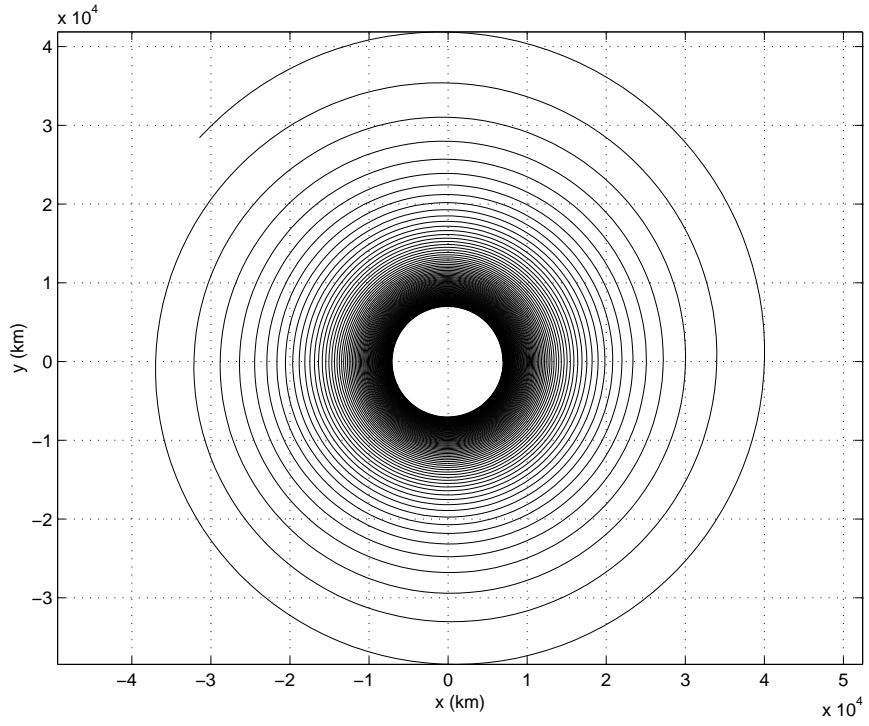


Figure 2 Case A Q-law transfer using a relative effectivity cut-off of $\eta_{r\text{ cut}} = 0$.

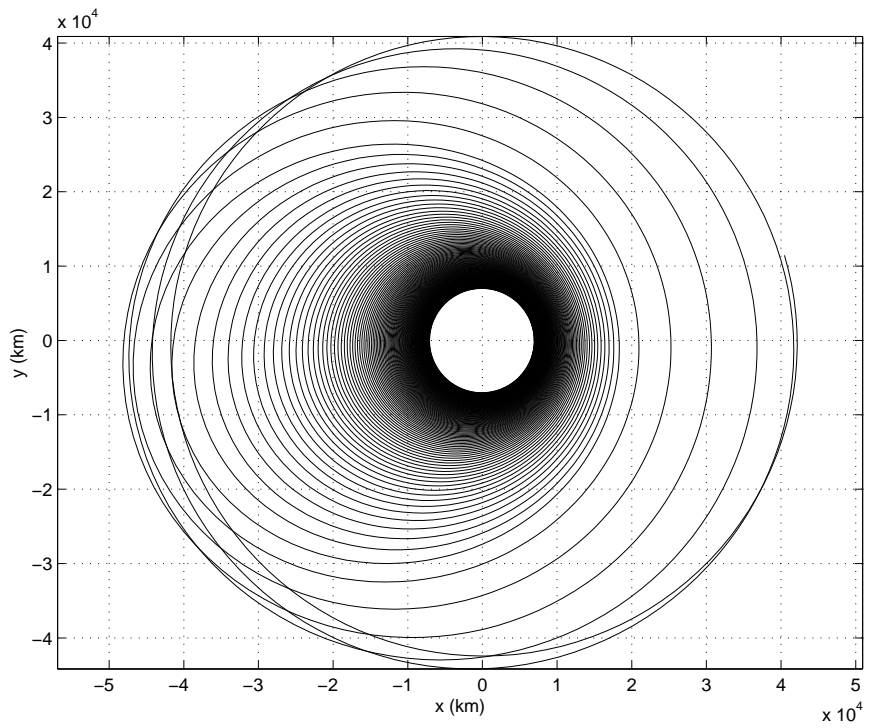


Figure 3 Case A Q-law transfer using a relative effectivity cut-off of $\eta_{r\text{ cut}} = 0.167$.

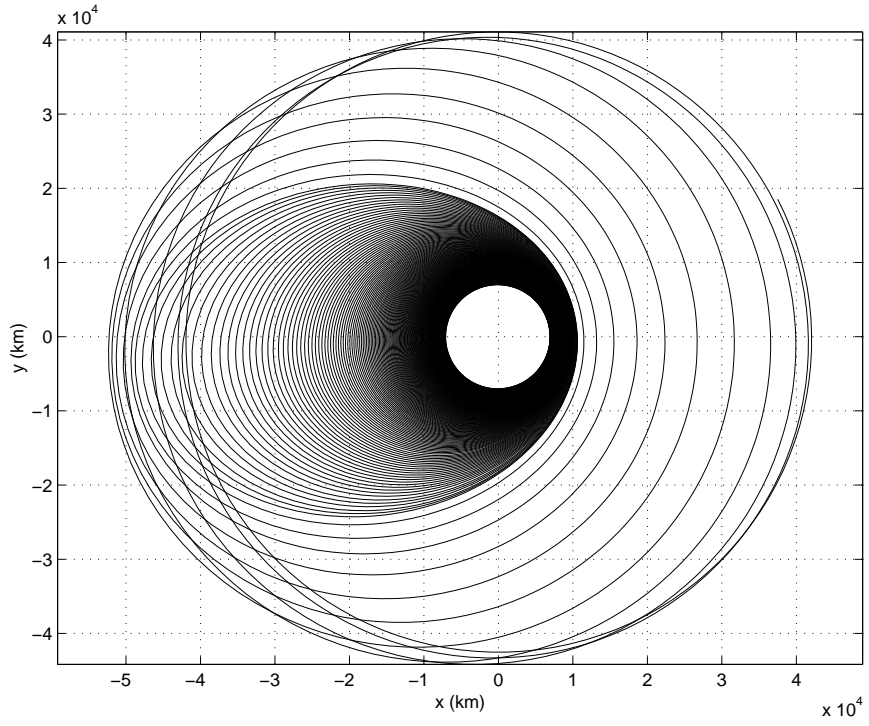


Figure 4 Case A Q-law transfer using a relative effectivity cut-off of $\eta_{r\text{ cut}} = 0.435$.

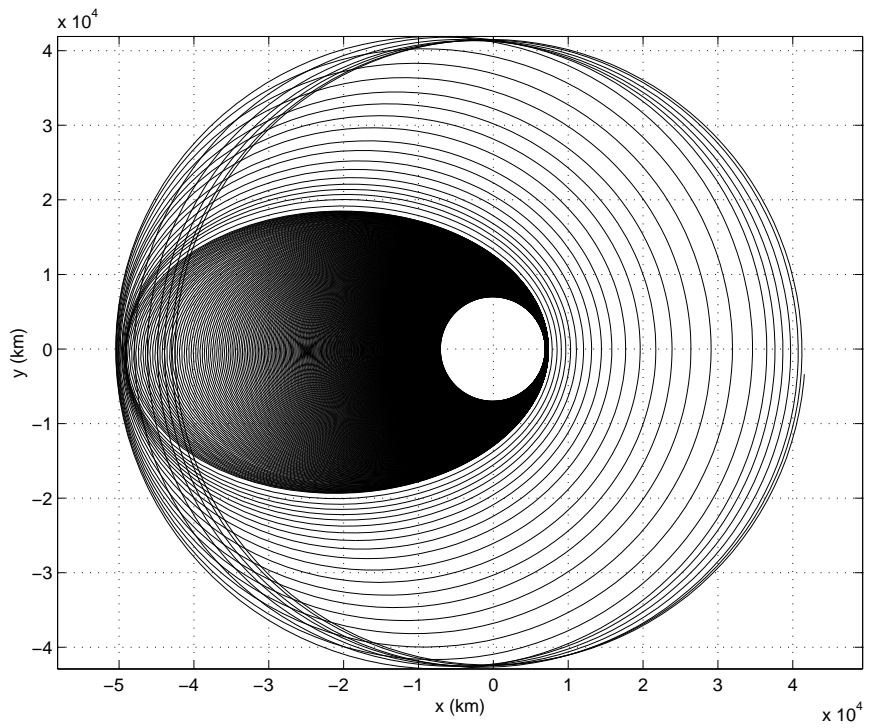


Figure 5 Case A Q-law transfer using a relative effectivity cut-off of $\eta_{r\text{ cut}} = 0.861$.

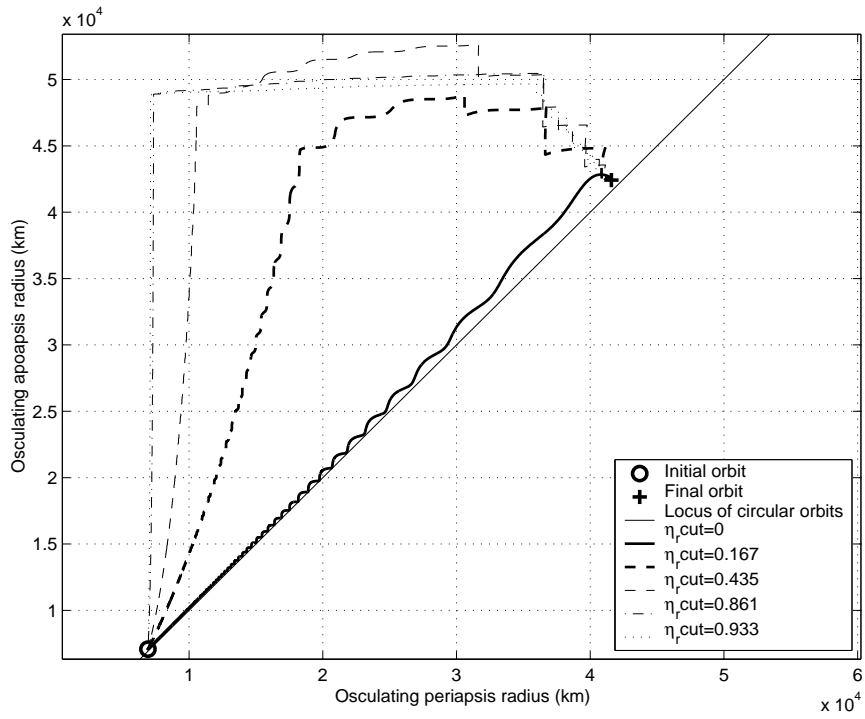


Figure 6 Case A Q-law transfers: Osculating values of apoapsis and periapsis radii for the five transfers corresponding to relative effectivity cut-off values ($\eta_{r\text{ cut}}$) of 0, 0.167, 0.435, 0.861, and 0.933.

appear in just the right directions and at just the right locations on the osculating orbit, so that most of the large, required change in ω is obtained within the first few revolutions of the transfer.

The present, refined definition of Q takes into account the fact that it is easier to change ω when i is close to 0 or 180 degrees. Thus, for the present transfer, in a balanced way and at the very beginning of the transfer, the Q-law will drive down i so as to change ω . The success of this strategy is evident in Fig. 7, where the propellant requirement for the refined Q-law (labelled as family N) lies below that of the old Q-law for all flight times. Additionally, the trade-off between propellant mass and flight time is “well-behaved” in that it is relatively smooth and continuous.

Data for the $\eta_{a\text{ cut}}$ values annotated in Fig. 7 are shown in Table 3. In addition, the time history of the orbit elements and of the consumed propellant mass are shown for each of these transfers in Fig. 8. A common characteristic of the transfers is the initial growth in r_a and the performance of the bulk of the inclination change at high values of r_a . In the longer flight time cases, r_a is built-up more slowly (over more revolutions), and therefore more efficiently in terms of propellant. Another common characteristic is that ω and Ω show large changes very early in the transfer. Because of the ease of changing these angular quantities early in the transfer when i is small, some of the changes take the angles to values that are approximately within multiples of 360° of the target values. For example, for ω , whose target value is 270° , the initial jumps in the value of ω are to values near 270° , -90° , and -450° .

The thrust angles as functions of the number of revolutions in true anomaly are shown in Figs. 10 and 11 for $\eta_{a\text{ cut}} = 0$, and in Figs. 12 and 13 for $\eta_{a\text{ cut}} = 0.652$. The latter figures also serve as guides to predict the true anomalies where thrust arcs will occur at other non-zero values of $\eta_{a\text{ cut}}$. For larger values, the thrust arcs will shrink in size, but will remain centred roughly at the same true anomalies and will retain similar thrust directions. For smaller values, the thrust arcs will expand in size, but again the location and direction of thrust will remain similar.

Table 3

Selected Q-law orbit transfer solutions for Case E

| $\eta_{a\text{ cut}}$ | Flight time (days) | ΔV (km/s) | Propellant Mass (kg) | Revs ^a |
|-----------------------|-----------------------|----------------------|-------------------------|-------------------|
| 0 | 81.61 | 8.738 | 719.012 | 114.38 |
| 0.652 | 149.79 | 6.143 | 537.808 | 214.01 |
| 0.909 | 296.77 | 5.495 | 488.695 | 429.98 |
| 0.966 | 501.45 | 5.394 | 480.896 | 724.49 |

^aRevolutions in true anomaly.

CONCLUSIONS

Based on Gauss’s form of the variational equations, and exploiting analytic expressions for the optimal thrust direction and location on the osculating orbit for changing each of the orbit elements except true anomaly, earlier work by the author presented a candidate Lyapunov function, the proximity quotient, Q , for performing low-thrust orbit transfers using Lyapunov feedback control. In the present work, Q has been modified slightly so as to permit the feedback control law (the Q-law) to capitalise on the ease of changing the argument of periapsis when inclinations are near 0 or 180 degrees. A relative effectivity cut-off for the thrust has also been introduced to simplify the examination of the trade-off between propellant mass and thrust, particularly for coplanar, circle-to-circle transfers. The improvements to the Q-law have been demonstrated by applying the refined

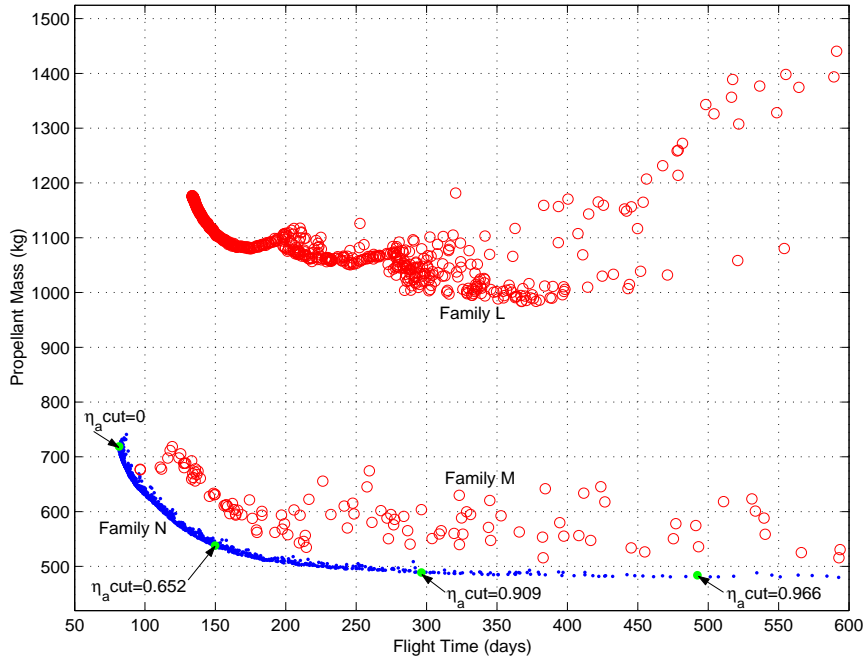


Figure 7 Case E Q-law transfer: Trade-off between propellant mass and flight time, assessed by varying and considering only the absolute effectivity cut-off, $\eta_{a \text{ cut}}$. Families L and M are obtained using the old definition for Q (as in Ref. ¹⁴), and Family N is obtained using the present refined definition for Q .

algorithm to a coplanar, circle-to-circle transfer and to a complex transfer from a geostationary transfer orbit to a retrograde, Molniya-type orbit, where the five orbit elements apart from true anomaly had target values. Being a feedback control algorithm, the Q-law is relatively simple to implement, runs very quickly, and permits a degree of disturbance rejection. Also, by virtue of the Lyapunov function chosen, Q , reasonable performance is obtained for a wide variety of transfers, meaning that a reasonable functional form has been found and that the optimisation of parameters within this functional form may lead to solutions that are very close to those found with traditional, direct and indirect trajectory optimisation techniques.

Acknowledgements

This research was carried out at the Jet Propulsion Laboratory, California Institute of Technology, under a contract with the National Aeronautics and Space Administration.

REFERENCES

1. Lawden, D. F., "Optimal Programming of Rocket Thrust Direction," *Astronautica Acta*, Vol.1, 1955, pp.41–56.
2. Edelbaum, T. N., "Optimum Power-Limited Orbit Transfer in Strong Gravity Fields," *AIAA Journal*, Vol.3, No.5, May 1965, pp.921–925.
3. Kechichian, J.A., "Optimal Low-Earth-Orbit-Geostationary-Earth-Orbit Intermediate Acceleration Orbit Transfer," *J. Guidance, Control, and Dynamics*, Vol.20, No.4, July-Aug. 1997, pp.803–811.
4. Geffroy, S. and Epenoy, R., "Optimal Low-Thrust Transfers with Constraints — Generalization of Averaging Techniques," *Astronautica Acta*, Vol.41, No.3, 1997, pp.133–149.

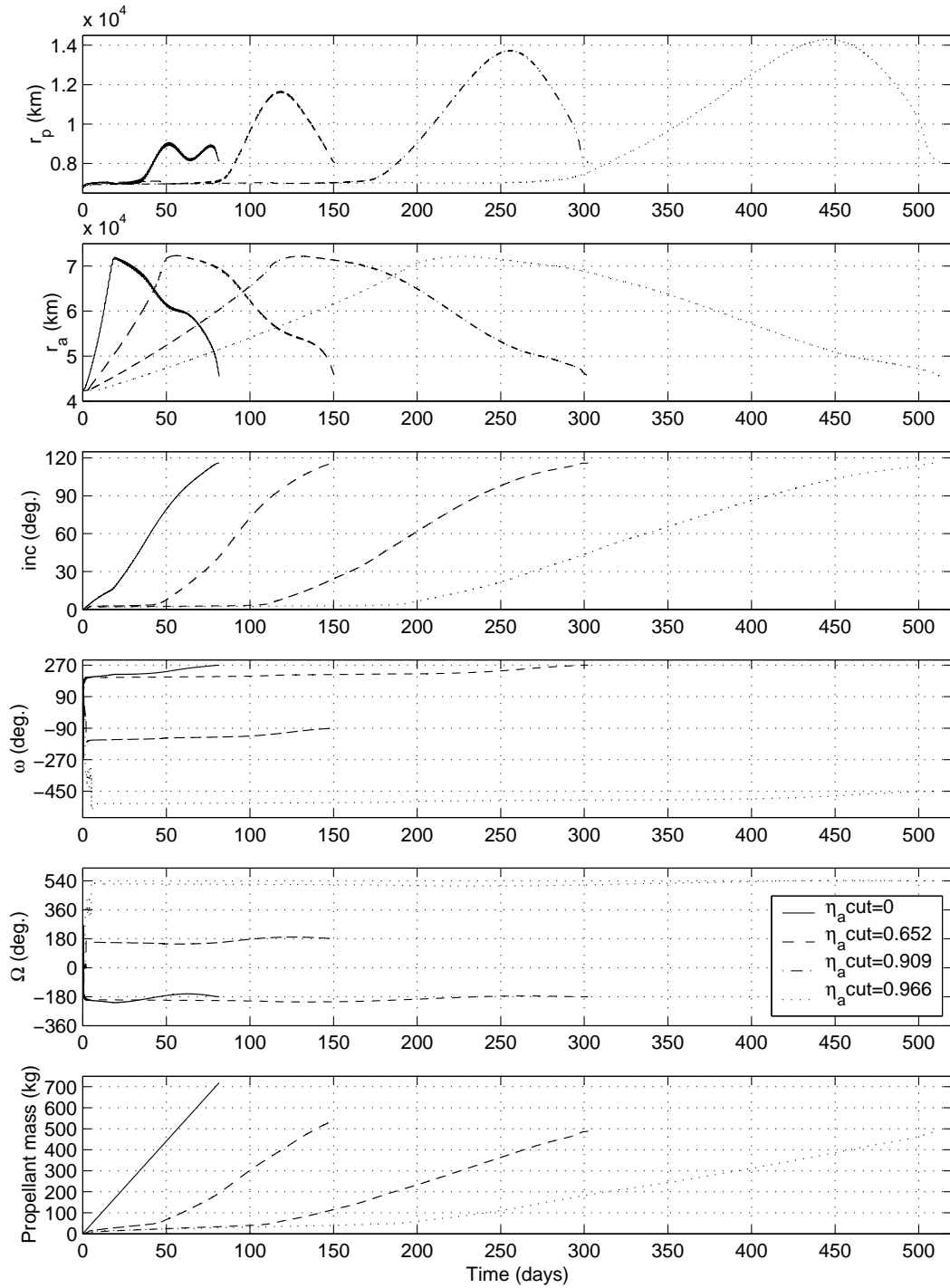


Figure 8 Case E Q-law transfer: Time history of orbit elements (periapsis radius, apoapsis radius, inclination, argument of periapsis, and longitude of the ascending node), and propellant mass consumed for four different transfers using different values of the absolute effectivity cut-off, $\eta_{a\text{cut}} = 0, 0.652, 0.909, \text{ and } 0.966$.

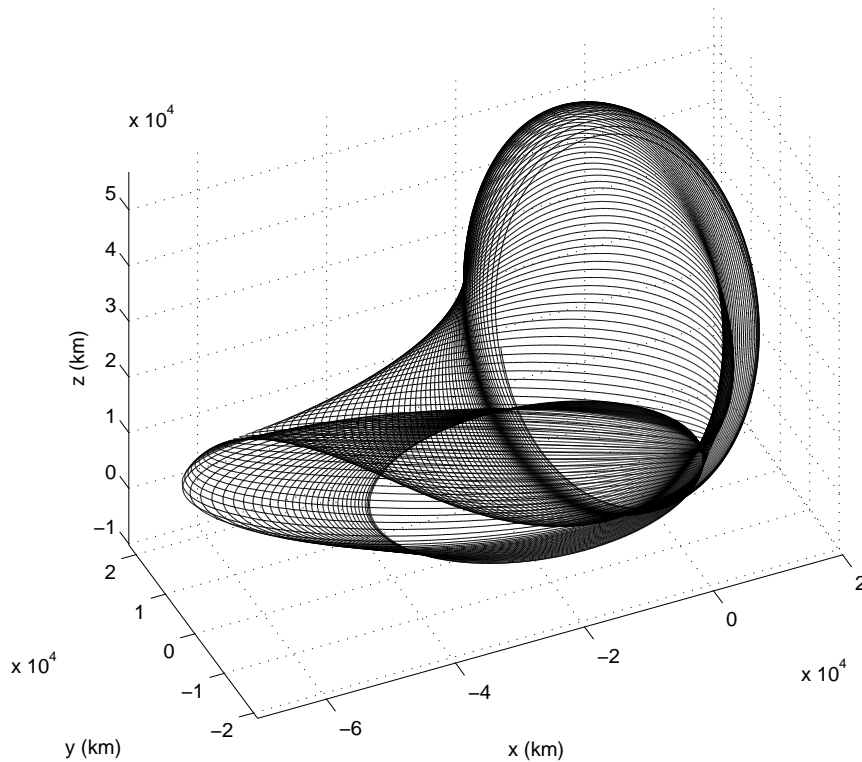


Figure 9 Case E Q-law transfer: Trajectory plot for $\eta_{a\text{cut}} = 0$.

5. Bishop, R.H. and Azimov, D.M., "Analytical space trajectories for extremal motion with low-thrust exhaust-modulated propulsion," *J. Spacecraft and Rockets*, Vol.38, No.6, Nov-Dec 2001, pp.897-903.
6. Whiting, J.K., "Three-dimensional low-thrust trajectory optimization, with applications," 39th AIAA/ASME/SAE/ASEE Joint Propulsion Conference and Exhibit, AIAA Paper 2003-5260, Huntsville, Alabama, July 20-23, 2003.
7. Kluever, C. A. and Oleson, S. R., "A Direct Approach for Computing Near-Optimal Low-Thrust Transfers," AAS/AIAA Astrodynamics Specialist Conference, AAS Paper 97-717, Sun Valley, Idaho, Aug. 4-7, 1997.
8. Chilan, C.M. and Conway, B.A., "Optimal Low-Thrust Supersynchronous-to-Geosynchronous Orbit Transfer," Paper AAS 03-632, AAS/AIAA Astrodynamics Specialist Conference, Big Sky, Montana, 03-07 Aug. 2003.
9. Whiffen, G. J. and Sims, J. A., "Application of a Novel Optimal Control Algorithm to Low-Thrust Trajectory Optimization," AAS/AIAA Space Flight Mechanics Meeting, AAS Paper 01-209, Santa Barbara, California, Feb. 11-15, 2001.
10. Whiffen, G.J., "Optimal Low-Thrust Orbit Transfers around a Rotating Non-Spherical Body" AAS/AIAA Space Flight Mechanics Meeting, AAS Paper 04-264, Maui, Hawaii, Feb. 8-12, 2004.
11. Kluever, C. A., "Simple Guidance Scheme for Low-Thrust Orbit Transfers," *J. Guidance, Control, and Dynamics*, Vol.21, No.6, Nov. 1998, pp.1015-1017.
12. Gefert, L. P. and Hack, K. J., "Low-Thrust Control Law Development for Transfer from Low Earth Orbits to High Energy Elliptical Parking Orbits," AAS/AIAA Astrodynamics Specialist Conference, AAS Paper 99-410, Girdwood, Alaska, Aug. 1999.
13. Petropoulos, A.E., "Simple Control Laws for Low-Thrust Orbit Transfers," AAS Paper 03-630, AAS/AIAA Astrodynamics Specialist Conference, Big Sky, Montana, 03-07 Aug. 2003.
14. Petropoulos, A.E., "Low-Thrust Orbit Transfers Using Candidate Lyapunov Functions with a Mechanism for Coasting," AIAA 2004-5089, AIAA/AAS Astrodynamics Specialist Conference, Providence, Rhode Island, 16-19 Aug. 2004.
15. Ilgen, M.R., "Low thrust OTV guidance using Liapunov optimal feedback control techniques," AAS/AIAA Astrodynamics Specialist Conference, AAS Paper 93-680, Victoria, Canada, 16-19 Aug 1993.

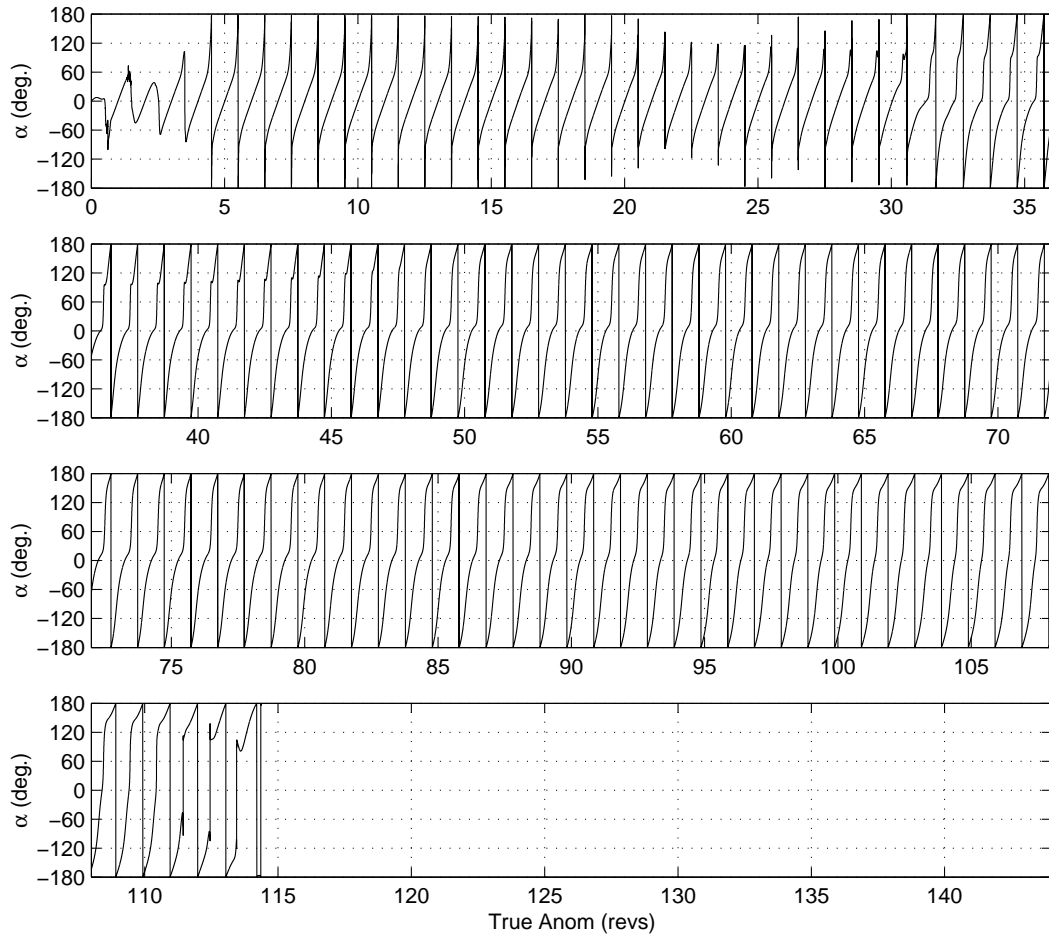


Figure 10 Case E Q-law transfer, $\eta_{a\text{cut}} = 0$: Evolution of the thrust angle α as a function of revolutions in true anomaly.

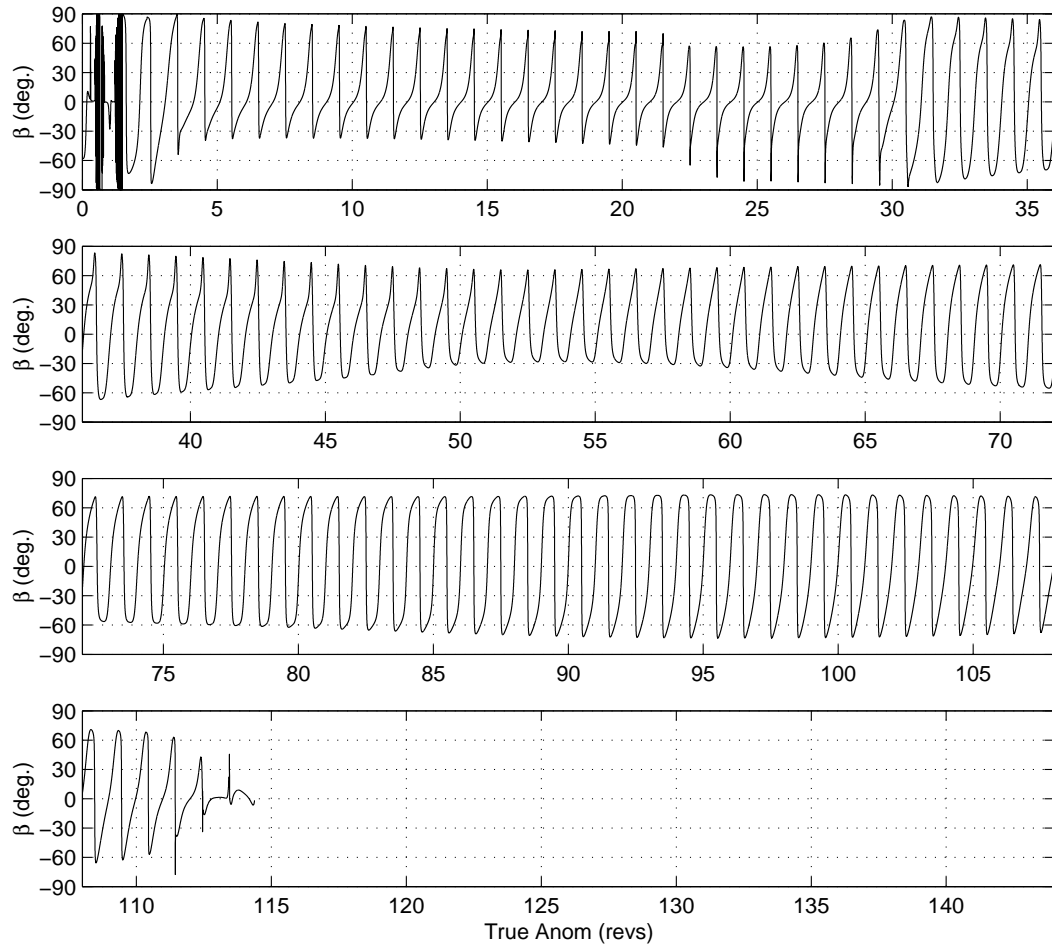


Figure 11 Case E Q-law transfer, $\eta_{a\text{cut}} = 0$: Evolution of the thrust angle β as a function of revolutions in true anomaly.

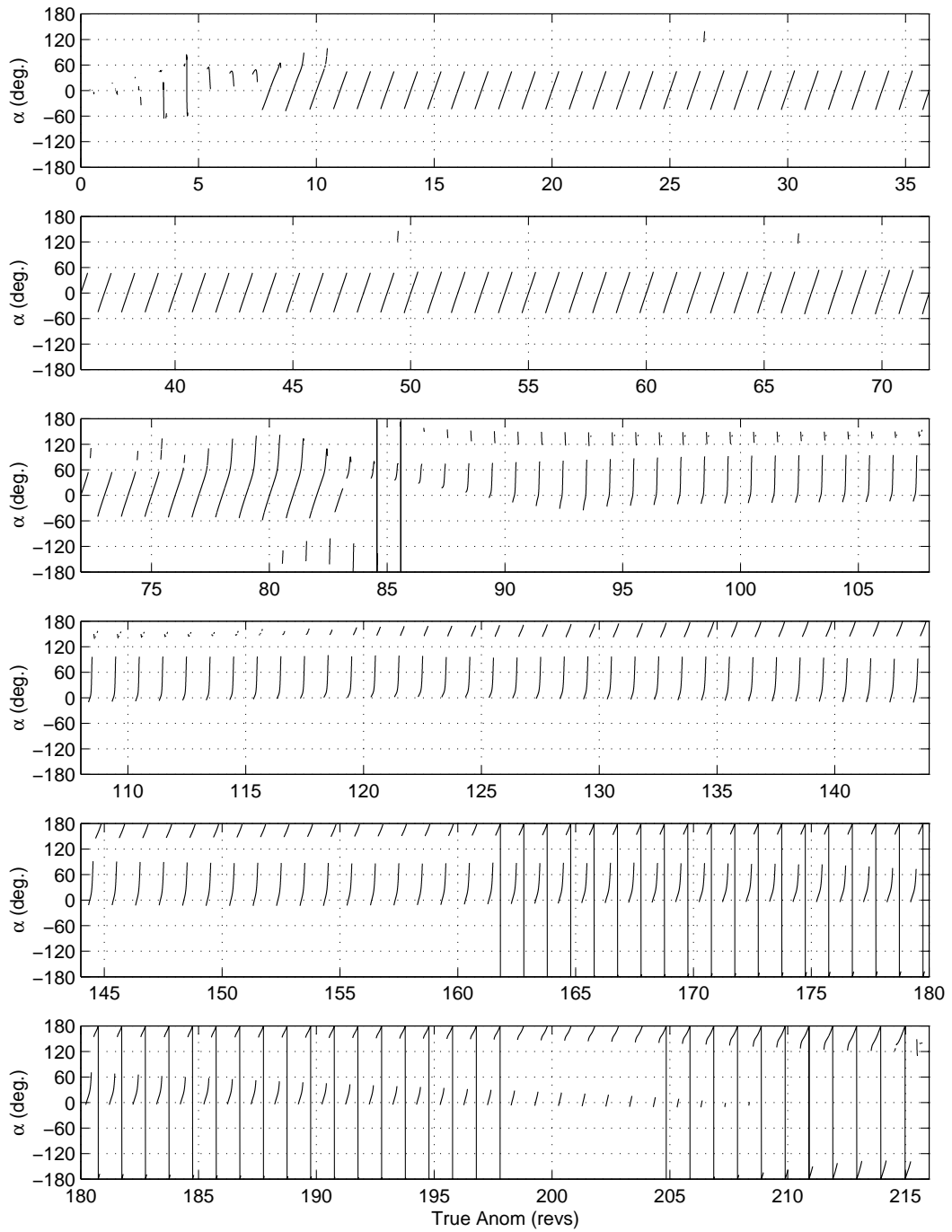


Figure 12 Case E Q-law transfer, $\eta_{a\text{cut}} = 0.652$: Evolution of the thrust angle α as a function of revolutions in true anomaly. Gaps in the plot correspond to coast periods (where no thrust is applied).

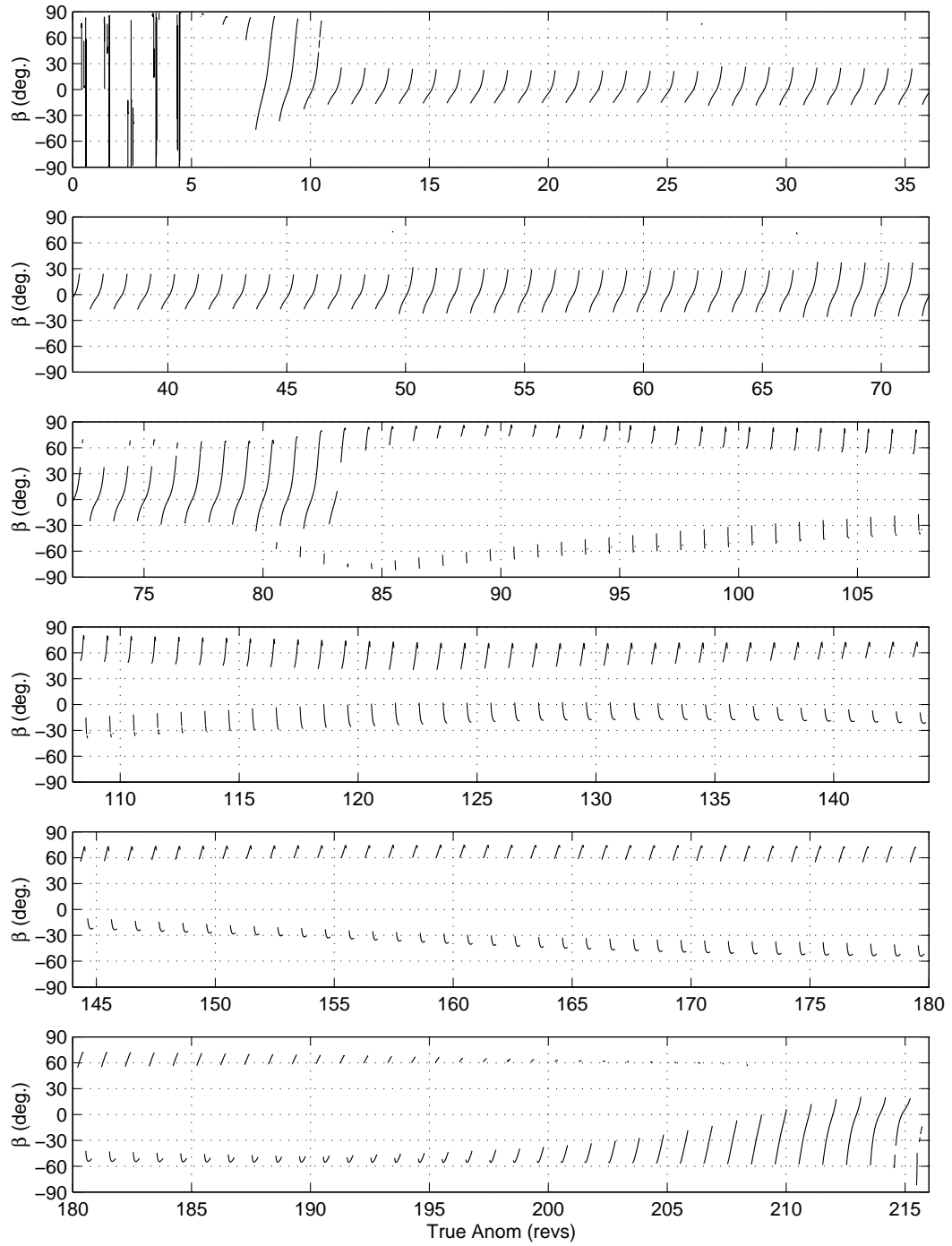


Figure 13 Case E Q-law transfer, $\eta_{a\text{cut}} = 0.652$: Evolution of the thrust angle β as a function of revolutions in true anomaly. Gaps in the plot correspond to coast periods (where no thrust is applied).

16. Chang, D.E., Chichka, D.F., Marsden, J.E., “Lyapunov functions for elliptic orbit transfer,” AAS/AIAA Astrodynamics Specialist Conference, AAS Paper 01-441, Québec City, Canada, July 30-Aug. 2 2001.
17. Battin, R. H., *An Introduction to the Mathematics and Methods of Astrodynamics*, 1st ed. 4th printing, AIAA, New York, 1987, pp.488–489.
18. Lee, S., von Allmen, P., Fink, W., Petropoulos, A.E., and Terrile, R., “Design and Optimization of Low-Thrust Trajectories,” accepted for presentation at the IEEE Aerospace Conference, Big Sky, Montana, 05-12 Mar. 2005.